The Journal of Maternal-Fetal & Neonatal Medicine

ISSN: (Print) (Online) Journal homepage: https://www.tandfonline.com/loi/ijmf20

Human placental microperfusion and microstructural assessment by intra-voxel incoherent motion MRI for discriminating intrauterine growth restriction: a pilot study

Amanda Antonelli, Silvia Capuani, Giada Ercolani, Miriam Dolciami, Sandra Ciulla, Veronica Celli, Bernd Kuehn, Maria Grazia Piccioni, Antonella Giancotti, Maria Grazia Porpora, Carlo Catalano & Lucia Manganaro

To cite this article: Amanda Antonelli, Silvia Capuani, Giada Ercolani, Miriam Dolciami, Sandra Ciulla, Veronica Celli, Bernd Kuehn, Maria Grazia Piccioni, Antonella Giancotti, Maria Grazia Porpora, Carlo Catalano & Lucia Manganaro (2022): Human placental microperfusion and microstructural assessment by intra-voxel incoherent motion MRI for discriminating intrauterine growth restriction: a pilot study, The Journal of Maternal-Fetal & Neonatal Medicine, DOI: 10.1080/14767058.2022.2050365

To link to this article: https://doi.org/10.1080/14767058.2022.2050365

THE JOURNAL OF MATERNAL-FETAL & NEONATAL MEDICINE
https://doi.org/10.1080/14767058.2022.2050365

Taylor & Francis
Taylor & Francis Group

ORIGINAL ARTICLE

Human placental microperfusion and microstructural assessment by intravoxel incoherent motion MRI for discriminating intrauterine growth restriction: a pilot study

Amanda Antonelli[a]*, Silvia Capuani[b]*, Giada Ercolani[a], Miriam Dolciami[a], Sandra Ciulla[a], Veronica Celli[a], Bernd Kuehn[c], Maria Grazia Piccioni[d], Antonella Giancotti[d], Maria Grazia Porpora[d], Carlo Catalano[a] and Lucia Manganaro[a]

[a]Department of Radiological, Oncological and Pathological Sciences, "Sapienza" University of Rome, Rome, Italy; [b]Physics Department, CNR Institute for Complex Systems (ISC), "Sapienza" University of Rome, Rome, Italy; [c]Siemens Healthcare GmbH, Erlangen, Germany; [d]Department of Gynaecological-Obstetrical and Urological Sciences, "Sapienza" University of Rome, Rome, Italy

ABSTRACT

Objectives: To evaluate the potential of Intravoxel Incoherent Motion (IVIM) Imaging in the quantification of placental micro-perfusion and microstructural features to identify and discriminate different forms of intrauterine growth restriction (IUGR) and normal fetuses pregnancies.

Methods: Small for gestational age SGA ($n = 8$), fetal growth restriction FGR ($n = 10$), and normal ($n = 49$) pregnancies were included in the study. Placental Magnetic Resonance Imaging (MRI) was performed at 1.5 T using a diffusion-weighted sequence with 10 *b*-values. IVIM fractional perfusion (fp), diffusion (D), and pseudodiffusion (D*) were evaluated on the fetal and maternal placental sides. Correlations between IVIM parameters, Gestational Age (GA), Birth Weight (BW), and the presence or absence of prenatal fetoplacental Doppler abnormalities at the US were investigated in SGA, FGR, and normal placentae.

Results: fp and D* of the placental fetal side discriminate between SGA and FGR ($p = .021$; $p = .036$, respectively), showing lower values in FGR. SGA showed an intermediate perfusion pattern in terms of fp and D* compared to FGR and normal controls. In the intrauterine growth restriction group (SGA + FGR), a significant positive correlation was found between fp and BW ($p < .002$) in the fetal placenta and a significant negative correlation was found between D and GA in both the fetal ($p < .0009$) and maternal ($p < .006$) placentas.

Conclusions: Perfusion IVIM parameters fp and D* may be useful to discriminate different micro-vascularization patterns in IUGR being helpful to detect microvascular subtle impairment even in fetuses without any sign of US Doppler impairment *in utero*. Moreover, fp may predict fetuses' body weight in intrauterine growth restriction pregnancies. The diffusion IVIM parameter D may reflect more rapid microstructural rearrangement of the placenta due to aging processes in the IUGR group than in normal controls.

ARTICLE HISTORY
Received 16 May 2021
Revised 7 January 2022
Accepted 3 March 2022

KEYWORDS
MRI; placenta; IUGR; IVIM; perfusion

1. Introduction

The human placenta is a highly perfused tissue with a complex microstructure and crucial physiological functions, allowing interchanges between maternal and fetal circulation and supporting fetal physiological growth [1,2]. Placental vascular dysfunction with impaired maternal-fetal circulation is the most frequent cause of intrauterine growth restriction (IUGR) [3–8]. IUGR is a leading cause of stillbirth, and it is highly associated with premature birth and lower perinatal and postnatal outcomes, with lifelong morbidity [9–12].

IUGR is challenging to define, and no gold standard for the diagnosis exists. It is usually defined by the statistical deviation of fetal size from a population-based reference, with a threshold at the 10th or 3rd centile. According to the criteria of the Delphi Consensus [13] growth-restricted fetuses may be differentiated into early onset and late onset (threshold: 32 weeks) and classified considering the presence or absence of functional parameters, either as solitary (absent end-diastolic flow in the umbilical artery UA) or contributory parameters (UA-PI or uterine artery UtA-PI > 95th centile or cerebroplacental ratio CPR < 5th centile) [13]. The prenatal US with feto-placental Doppler is considered the primary diagnostic tool in these conditions. Current evidence shows that there

CONTACT Silvia Capuani silvia.capuani@isc.cnr.it NMR and Medical Physics Laboratory, Physics Department, CNR Institute for Complex Systems (ISC), "Sapienza" University of Rome, Piazzale Aldo Moro, 5, Rome, 00185, Italy
*These authors contributed equally to this work.

are two main prenatal forms of growth restriction: fetal growth restriction (FGR) with abnormalities in feto-placental Doppler and a higher risk for *in utero* deterioration/stillbirth; and small for gestational age (SGA) fetuses, generally considered "constitutionally small," without evident changes in feto-placental Doppler and near normal perinatal outcomes [14–20]. However, recent literature shows that both fetuses with or without UA Doppler changes have suboptimal perinatal outcomes and a certain form of placental dysfunction [18–20]. In this view, US examination with the fetoplacental Doppler study might lead to an underestimation of perinatal outcome in those considered constitutional small fetuses. US examination alone may also have limitations from a microscopic perspective, showing itself not measuring perfusion in-depth, and microvascularization quantification remains unclear [21,22]. Therefore, the development of new non-invasive imaging techniques more suited to detect subtle placental changes indicating premature pathological aging [23] is highly desirable for proper perinatal management.

Prenatal Magnetic Resonance Imaging (MRI) with Diffusion-weighted imaging (DWI) has improved its role in the *in vivo* study of the human placenta and fetal growth [24–29]. In particular, IntraVoxel Incoherent Motion (IVIM) imaging [30] with a bi-exponential model of diffusion allowing the independent quantification of perfusion and diffusion qualities has been recently adapted to prenatal imaging studies showing high potential diagnostic ability [31–35]. Some studies highlighted the ability of IVIM to discriminate between normal and IUGR pregnancies [36,37]. In this study, we hypothesized that the IVIM model might differentiate between the placental pattern of microvascularization and tissue microstructure of SGA and FGR. The present study aimed to identify potential biomarkers of SGA and FGR pregnancies. Toward this goal, we (i) quantified IVIM parameters of diffusion and perfusion in normal, SGA, and FGR pregnancies, and (ii) studied correlations between IVIM parameters obtained in different areas of the fetal and maternal placenta, gestational age (GA), and birth weight (BW).

2. Methods

2.1. Subjects

One hundred twenty-three singleton pregnancies were consecutively and prospectively enrolled to undergo placental MR in our Radiology Department between January 2017 and January 2020. Written informed consent from the mother was obtained in all cases, and the study was approved by the local Ethics Committee. Information about the presence or absence of fetoplacental Doppler abnormalities at prenatal US assessment was collected. US morphological examination to assess Estimated Fetal Weight (EFW) and fetoplacental circulation with feto-placental Doppler examination was performed in all pregnancies one week before the MR examination. GA was assessed by the last menstrual period (LMP) and confirmed by first-trimester ultrasound CRL.

Pregnancies with fetal pathologies, such as congenital infections and with fetal growth restriction correlated with malformations were not considered for the study sample. Placental insertion or invasion pathologies were not included in the study sample. Mothers affected by preexisting chronic morbidities (i.e. diabetes, coagulation disorders, auto-immune pathologies) were also excluded.

Regarding the pathological group, pregnancies with an indication of placental MRI for a US detection of growth restriction were enrolled. Fetuses were classified according to the Deplhi consensus [13] as growth-restricted with a reduction of EFW with a threshold at the 10th or 3rd centile. In our cohort, fetuses were considered FGR with a low EFW and/or fetoplacental Doppler anomalies (uterine artery PI $<$ 95th percentile), while fetuses were considered SGA with a low EFW without fetoplacental Doppler impairment (uterine artery PI $>$ 95th percentile. The majority of SGA fetuses were late onset IUGR ($\geq$32 weeks). Regarding the selection of the control group, consecutive fetal MR of patients with a normal delivery at term ($>$37 weeks of gestation) and an appropriate EFW, Doppler study, and BW for the standard reference [9], without maternal or fetal pathologies, were recruited. Indications to MR examination were inadequate morphological US examination due to maternal habitus and/or fetal position, previous pathological pregnancies, suspected placenta accreta, borderline Ventriculomegaly, inadequate US visualization, or suspected anomaly of cavum septi pellucidi, suspected corpus callosum dysgenesis, and suspected posterior cranial fossa anomalies. All MR examinations were negative for fetal or placental abnormalities.

2.2. MR protocol

Placental MR examinations without maternal-fetal sedation were performed on a Siemens MAGNETOM Avanto 1.5 T scanner (Siemens Healthcare GmbH) using a supine position with feet first modality and two Body Matrix Coils on the maternal abdomen.

A conventional placental MR protocol was performed to visualize myometrium and placenta and to depict placental position, umbilical cord insertion, and parenchymal signal intensity characteristics. The MRI protocol included T2-HASTE (Half Fourier Single-shot Turbo Spin Echo) Weighted Imaging (WI) with and without Fat Suppression (FS) and TrueFISP WI in para-coronal, para-axial, and sagittal planes on the maternal uterus. T1 WI with and without FS on sagittal and para-axial planes was added to depict hemorrhagic lacunae's presence.

The IVIM protocol included diffusion-weighted (DW) Echo-Planar Imaging (EPI) sequence on the para-axial plane on maternal uterus including the whole placental surface, with TR/TE = 4000 ms/79 ms; bandwidth = 1628 Hz/px; matrix-size = 192×192; number of slices = 30; in-plane resolution = $2.0 \times 2.0\,mm^2$ and slice thickness = 4 mm. The diffusion encoding gradients were applied along three directions (x, y, z) using ten different b-values (0, 10, 30, 50, 75, 100, 150, 400, 700, and $1000\,s/mm^2$). The center of the field of view (FOV) was placed in the umbilical insertion area. The number of averages signal (NS) was NS = 2 for DW images acquired at b-value below $b = 150\,s/mm^2$ and NS = 4 for DW images acquired at b-value 400, 700, and $1000\,s/mm^2$. Due to fetal movements during the MR examination, low signal-to-noise ratio (SNR) of DWIs and the inadequate amount of data at low b-values (i.e. $b < 150\,s/mm^2$) are obvious drawbacks to extract reliable IVIM parameters. Therefore, we carefully selected b-values and the number of the averaged signal (NS) as a compromise between the number of b-values, NS value, and the exam duration. The duration of the IVIM acquisition was about 6 min.

2.3. MRI pre-processing

Two radiologists with sixteen and seven years of experience in prenatal MRI performed the image quality selection. Investigators who analyzed the MRI data were blind to fetal and placental conditions. Since the reliability of IVIM measurements depends on the SNR of DWI, SNRs of DW images acquired at b-value equal to 0 and $1000\,s/mm^2$ were evaluated. To estimate the SNR, an area in the placenta (to compute the signal) and an area placed outside the subject's body (to compute the background noise) were selected, and the ratio between the mean of the signal and the standard deviation (SD) of the noise, times 0.655, was obtained. The 0.655 factor is due to the Rician distribution of the background noise in a magnitude MR image. The average value of SNR over a cohort of ten subjects was then computed. The mean SNR at $b = 1000\,s/mm^2$ was 10 ± 3, which is an entirely acceptable value for considering DW data reliable [38]. These values guarantee no-biased IVIM values.

2.4. IVIM analysis

DICOM images of DWI acquisitions were elaborated offline with a prototype software named 'Siemens MR Body Diffusion Toolbox' to obtain fractional perfusion (fp), diffusion (D), and pseudodiffusion (D*) maps. Signal intensity was averaged in each selected ROI (maternal and fetal side placenta), and the function:

$$S(b)/S(0) = fp\ \exp(-b\ D*) + (1 - fp)\ \exp(-b\ D) \quad (1)$$

where S(b) is the diffusion-weighted signal and S(0) is the signal at $b = 0\,s/mm^2$ was fitted to data. The first part of the bi-exponential curve displayed in Equation (1) describes the perfusion compartment with a rate quantified by the pseudo-diffusion coefficient D*, and the perfusion fraction fp quantifies the fraction of water molecules pseudo-diffusing. The second part of the Equation (1) describes the diffusion, with a diffusion coefficient D due to $(1 - fp)$ water molecules. In the placental tissue, fp quantifies the perfusion fraction of water molecules perfused in microcapillaries with D* rate, whereas D, quantifying hindered diffusion of water molecules in the extracellular space, is related to tissue microstructure.

2.5. Statistical analysis

The differences between mean values of D, D*, and fp in the two investigated ROIs (maternal and fetal placenta) of the normal, SGA, and FGR groups were assessed with the Analysis of Variance (ANOVA) test with Bonferroni correction for multiple comparisons. A Pearson test with Bonferroni correction was performed to investigate the linear correlation between D, D*, f, and GA and BW. All statistical analysis was performed using SPSS Statistics 20 (IBM SPSS, Inc. Chicago, IL, USA). Moreover, to estimate the short-term reproducibility of IVIM measurement, we calculated for each IVIM parameter (D, D*, and fp) the coefficient of variation (CV) defined as the ratio of the standard deviation SD to the mean, using the mean and the SD of two consecutive acquisitions obtained in three volunteers (belonging to the normal control group).

3. Results

3.1. Subjects

Due to fetal movement artifacts, 17% of DWI acquisitions were discarded. Twenty-nine examinations were discarded for the further detection of co-existing fetal pathology causing IUGR. Four pregnancies were excluded for further detection of normal fetal growth without EFW or Doppler impairment. Two subjects were excluded from the study sample due to stillbirth.

The total study sample was then composed of 67 subjects. Growth restriction was postnatally confirmed with a BW below the 10th percentile compared to the standard reference. The final pathological cohort was composed of 18 IUGR pregnancies, 10 FGR with fetoplacental Doppler abnormalities, and 8 SGA with normal Doppler fetal-maternal circulation. No hypertension pre-eclampsia was observed in the selected subjects. The final control group was composed of 49 pregnancies. Additional information on the clinical characteristics of the study subgroups is described in Table 1.

3.2. IVIM analysis

CV of fp was ~3% (range 1.4–4.4%) in the fetal placenta and 3% (range 0.4–4.5%) in the maternal placenta. Moreover, CV of D* and D in fetal placenta were 5% (range 2–9%) and 1% (range 0.7–2%), respectively, whereas CV of D* and D in maternal placenta were 6% (range 0.6–9%) and 0.5% (range 0.2–1%), respectively.

The IVIM parameter fp allowed the discrimination of SGA from FGR, showing significantly higher mean values in the SGA fetal ROI ($p = .021$). The same behavior was observed considering D* ($p = .036$). SGA placentae showed intermediate fp mean values compared to the FGR subgroup and normal controls (Table 2).

FGR subjects showed statistically significant lower values of fp and D* compared to controls, in both fetal (fp: $p = 1.1{*}10^{-9}$; D*: $p = .009$) and maternal side (fp: $p = 8.4{*}10^{-5}$; D*: $p = 1.6{*}10^{-5}$). On the other hand, SGA showed statistically significantly lower values of fp than controls, with significantly lower mean values of fp in both fetal ($p = 3.8{*}10^{-7}$) and maternal side ($p = .001$).

A statistically significant positive correlation was found between fp and BW in the fetal placenta of the pathological IUGR (FGR + SGA) group. Lower fp mean values were associated with lower weight at birth (Figure 1(A)). In the IUGR (FGR + SGA) group, a significant decreasing behavior of D values during gestation was found in both fetal and maternal side ROIs (Figures 1(B,C)). Conversely, no significant correlation was found between D and GA in normal placentas.

4. Discussion

In vivo placental microstructural and perfusion impairment occurring in fetal smallness is poorly understood, and identifying imaging biomarkers to quantify placental development *in utero* for better management of high-risk pregnancies is highly desirable. The US with fetoplacental flowmetry is useful to detect macroscopic vascular impairment in IUGR placentae, but it cannot study placental parenchyma microstructural and microvascular characteristics. In current literature, placental microstructure study through IVIM is a discussed topic [26,31,33,36,37,39–42], especially due to

Table 1. Clinical characteristics of the study population.

	FGR ($n = 10$)	SGA ($n = 8$)		p FGR *vs.* SGA	p Normal *vs.* FGR	p Normal *vs.* SGA
GA at MRI (weeks)	**26.5 (±4.5)**	32.0 (±4.9)	**31.1 (±5.2)**	NS	0.045	NS
Maternal age (years)	32 (±5.6)	31 (±5.5)	30 (±5.7)	NS	NS	NS
BMI (kg/m^2)	24.8 (±2.8)	25.2 (±4.3)	24.7 (±3.2)	NS	NS	NS
GA at Delivery (weeks)	**35.6 (±2.6)**	**36.0 (±1.6)**	**39.0 (±1.6)**	NS	0.002	0.006
C-section (%)	47	43	39	–	–	–
Birth weight (g)	**2189 (±211)**	**2513 (±245)**	**3196 (±302)**	0.02	10^{-7}	$3{*}10^{-6}$
Male baby's sex (%)	60	50	44.9	–	–	–

p: p-value of ANOVA test.
Bold values indicate statistically different mean values.

Table 2. Comparison of IVIM parameters quantified in the fetal and the maternal placentas of Normal, FGR, and SGA group.

		FGR	SGA	Normal	p FGR *vs.* SGA	p Normal *vs.* FGR	p Normal *vs.* SGA
Fetal	fp	**26.49 ± 1.98**	**29.01 ± 1.91**	**37.24 ± 6.86**	**0.021**	**$1.1{*}10^{-9}$**	**$3.8{*}10^{-7}$**
	D*	**21.57 ± 1.01**	**23.19 ± 1.65**	25.24 ± 6.49	**0.036**	**0.009**	NS
	D	1.45 ± 0.18	1.56 ± 0.24	1.29 ± 0.21	NS	NS	NS
Maternal	fp	**21.73 ± 2.82**	**23.58 ± 2.42**	**30.13 ± 5.73**	NS	**$8.4{*}10^{-5}$**	**0.001**
	D*	**17.82 ± 1.11**	18.51 ± 2.70	**22.81 ± 5.61**	NS	**$1.6{*}10^{-5}$**	NS
	D	1.37 ± 0.16	1.50 ± 0.14	1.33 ± 0.17	NS	NS	NS

fp: perfusion fraction (%); D: diffusion coefficient (10^{-3}mm^2/s); D*: pseudo-diffusion coefficient ($\cdot 10^{-3}$mm^2/s); p: p-value of ANOVA test.
Bold values indicate statistically different mean values.

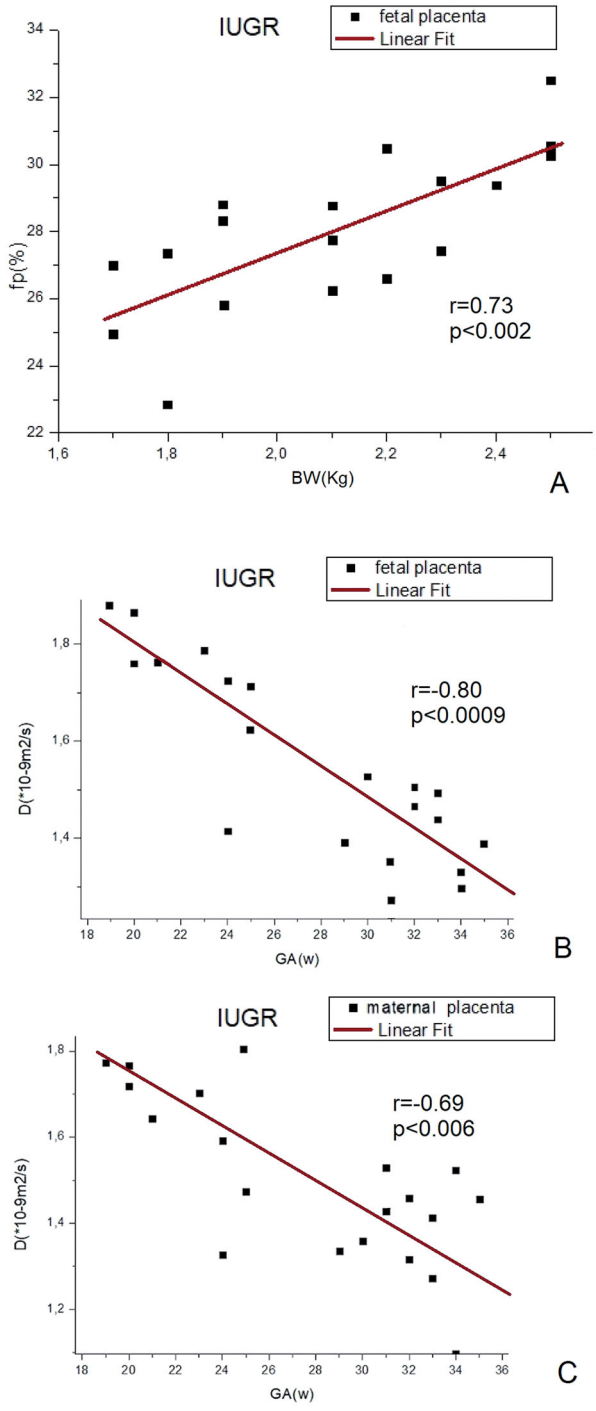

Figure 1. IUGR cohort. Scatter plot graph depicting the significant linear correlation between fp mean values and fetus body weight (BW) in fetal placenta side (A); D mean values against the gestational age (GA) in fetal ROI (B) and in maternal ROI (C) of the placenta. A significant decrease of D mean values during gestation aging is shown.

the potential of evaluating blood micro-perfusion through the IVIM fp parameter [43].

Our results are in substantial agreement with previous IVIM studies on normal and IUGR placentae, with a general decrease of fp in pathological parenchyma [31,36,37,39–43]. Nevertheless, in addition to these investigations, in this work, IVIM results suggest mild placental microperfusion impairment also in fetuses classified as SGA, who were negative for fetoplacental US Doppler abnormalities. We found three different patterns of parenchymal perfusion in terms of fp: SGA placentae showed an intermediate pattern of microperfusion compared to the FGR subgroup and normal controls, an expression of an intermediate grade of placental perfusion impairment, which is not as severe as FGR but not even completely into normal the range as control placentae. Indeed, a significant difference of fp between SGA and the normal group was found in both fetal and maternal placenta side even without US Doppler abnormalities differences.

The identification of growth-restricted fetuses at risk of adverse perinatal outcomes is challenging and a matter of debate in current literature, especially in late onset cases and when the UA Doppler (UA and UtA) commonly used in clinical practice cannot properly discriminate fetuses at higher risk of perinatal compromise [19]. More recently, assessment of blood flow in the umbilical vein (UV) has been shown to provide better identification of late-onset FGR fetuses at higher risk of perinatal compromise [19,44,45]. UV flow was also found to be impaired in late SGA fetuses without UA Doppler abnormalities [44]. Similarly, in our study, also in those considered constitutionally SGA, a subtle placental microperfusion impairment is present compared to normal placentae. Speculatively, fp may add useful information about the microperfusion of placental parenchyma when UA Doppler is normal, confirming that a proportion of fetal growth restriction with normal umbilical artery Doppler may still be explained by placental insufficiency, and the presence of subtle or initial placental insufficiency is not often reflected by UA Doppler.

Unlike the FGR group, which shows significant differences in both fp and D* values compared to the normal group, the SGA group shows significant differences compared to the normal group only for the perfusion fraction fp. Therefore, even if a limited number of SGA ($n = 8$) and FGR ($n = 10$) but a larger group of normal ($n = 49$) placentas were investigated, this work suggests that there is not only a decreased fraction of perfusion in micro-capillaries (quantified by fp) but also a decreased microcirculation rate (quantified by D*) in the FGR group compared to normal and SGA placentae. The combined significant decrease of fp and D* in FGR strengthens the hypothesis that FGR compared to SGA placentae is characterized by different and more consistent parenchymal impairment,

leading to perfusion anomalies. These results agree with observations that SGA and FGR human placentae histology show signs of accelerated placental aging, including lower telomerase activity and shorter telomeres within addition signs of apoptosis only for FGR [23,46,47].

In this work, IVIM fp and D* parameters may be potential biomarkers to identify different forms of placental parenchymal impairment occurring in IUGR (FGR + SGA), as they significantly discriminate between FGR and SGA group (Table 2). Moreover, fp positively correlates with BW of the IUGR group with the lower value of fp, the smaller the fetus, the higher value of fp, the bigger the fetus: thus, fp may have potentiality in predicting fetal BW.

In the pathological IUGR group, we found a negative correlation between D and GA on both maternal and fetal placenta sides, depicting a gradual and progressive increment of diffusion restriction with aging, as already suggested by previous investigations [37,40–43]. The D decrease may be in line with the progressive physiological involution of placental tissue with advanced GA. In this paper, we observed a more rapid decrease of D with GA in the IUGR group compared to no significant correlation between D and GA in normal placentae and results previously obtained in normal placentae [32], reflecting possible accelerated processes of senescence occurring in both FGR and SGA compared to normal placentae. This finding, together with a decreased fp, strengthens the hypothesis that IUGR placentae are characterized by microstructural impairment that leads to perfusion anomalies.

Although the present study is related to *in vivo* quantitative investigation that may differ from *ex vivo* results, we believe that our results are in agreement with *ex vivo* pathological findings described in the literature in both SGA and FGR placentae [23,46–49]. Moreover, in most placentas with normal UA Doppler, histological abnormalities secondary to maternal underperfusion have been described, reflecting latent insufficiency in uteroplacental blood supply [48], in agreement with the higher risk of adverse perinatal outcomes reported in this population. Placental parenchyma in both SGA and FGR seems to be characterized by various degrees of structural abnormalities with tissue heterogeneity, hypercellularity, and elevated deposition of fibrin by fibroblasts. These abnormalities may be responsible for the decrease in diffusion (quantified by IVIM parameter D) with the progress of gestation, which becomes increasingly restricted as the accumulation of fibrin and hypercellularity increases (Figures 1(B,C)). There are accelerated aging processes [23,46,47] with an increased occurrence of phenotypical structural abnormalities, such as thrombosis, ischemic and hemorrhagic infarction, and inflammatory changes [48–50]. In our opinion, an impaired intervillar environment may lead to a constriction of microperfusion, reducing fetoplacental exchanges [1–3,23,48–51]. These *ex vivo* findings may explain the significant reduction of perfusion values fp and D* in IUGR found in our cohort *in vivo* and the differences in fp and D* mean values between the SGA and FGR subgroups.

In conclusion, perfusion IVIM parameters fp and D* may be useful to discriminate different micro-vascularization patterns in different forms of IUGR, helping to detect microvascular subtle impairment even in fetuses without any sign of US Doppler impairment *in utero*. Moreover, fp may predict fetuses' body weight in intrauterine growth restriction pregnancies. The diffusion IVIM parameter D may reflect more rapid microstructural rearrangement of the placenta due to increased aging processes in the IUGR group than in normal controls.

4.1. Practical applications

FGR is not synonymous with SGA and noninvasive techniques to distinguish between them are needed. This work showed that IVIM placental MRI might have the potential to distinguish FGR from SGA and might predict IUGR body weight. The quantitative evaluation of microscopic perfusion and structural changes in dysfunctional placentae using IVIM may add useful information for a more in-depth understanding of different phenotypes of IUGR, improving the difficult perinatal prognosis of these pregnancies and being helpful for a proper postnatal prognostic assessment.

Disclosure statement

There are no known conflicts of interest associated with this publication and there has been no significant financial support for this work that could have influenced its outcome.

Funding

The author(s) reported there is no funding associated with the work featured in this article.

ORCID

Silvia Capuani http://orcid.org/0000-0002-7863-1801

References

[1] Benirschke K, Driscoll SG. The pathology of the human placenta BT. In: Strauss F, Benirschke K, Driscoll SG, editors. Placenta. Berlin; Heidelberg: Springer; 1967. p. 97–571.

[2] Serov AS, Salafia CM, Filoche M, et al. Analytical theory of oxygen transport in the human placenta. J Theor Biol. 2015;368:133–144.

[3] Regnault TRH, Galan HL, Parker TA, et al. Placental development in normal and compromised pregnancies—a review. Placenta. 2002;23:S119–S129.

[4] Barut F, Barut A, Gun BD, et al. Intrauterine growth restriction and placental angiogenesis. Diagn Pathol. 2010;5:24.

[5] Burton GJ, Jauniaux E. Pathophysiology of placental-derived fetal growth restriction. Am J Obstet Gynecol. 2018;218(2S):S745–S761.

[6] Lackman F, Capewell V, Gagnon R, et al. Fetal umbilical cord oxygen values and birth to placental weight ratio in relation to size at birth. Am J Obstet Gynecol. 2001;185(3):674–682.

[7] ISUOG practice guidelines: diagnosis and management of small-for-gestational-age fetus and fetal growth restriction. Ultrasound Obstet Gynecol. 2020; 56:298–312.

[8] McCowan LM, Figueras F, Anderson NH. Evidence-based national guidelines for the management of suspected fetal growth restriction: comparison, consensus, and controversy. Am J Obstet Gynecol. 2018;218(2):S855–S868.

[9] Villar J, Cheikh L, Ismail CG, et al. International fetal and newborn growth consortium for the 21st century (INTERGROWTH-21st), international standards for newborn weight, length, and head circumference by gestational age and sex: the newborn cross-sectional study of the INTERGROWTH-21st project. Lancet. 2014;384(9946):857–868.

[10] Baschat AA. Neurodevelopment following fetal growth restriction and its relationship with antepartum parameters of placental dysfunction. Ultrasound Obstet Gynecol. 2011;37(5):501–514.

[11] Gilchrist C, Cumberland A, Walker D, et al. Intrauterine growth restriction and development of the hippocampus: implications for learning and memory in children and adolescents. Lancet Child Adolesc Health. 2018;2(10):755–764.

[12] Larroque B, Bertrais S, Czernichow P, et al. School difficulties in 20-year-olds who were born small for gestational age at term in a regional cohort study. Pediatrics. 2001;108(1):111–115.

[13] Gordijn SJ, Beune IM, Thilaganathan B, et al. Consensus definition of fetal growth restriction: a Delphi procedure. Ultrasound Obstet Gynecol. 2016; 48(3):333–339.

[14] Figueras F, Gratacós E. Update on the diagnosis and classification of fetal growth restriction and proposal of a stage-based management protocol. Fetal Diagn Ther. 2014;36(2):86–98.

[15] Figueras F, Eixarch E, Gratacos E, et al. Predictiveness of antenatal umbilical artery doppler for adverse pregnancy outcome in small-for-gestational-age babies according to customised birthweight centiles: population-based study. BJOG. 2008;115(5):590–594.

[16] Richardus JH, Graafmans WC, Verloove-Vanhorick SP, et al. Differences in perinatal mortality and suboptimal care between 10 European regions: results of an international audit. BJOG. 2003;110(2):97–105.

[17] Gardosi J, Madurasinghe V, Williams M, et al. Maternal and fetal risk factors for stillbirth: population based study. BMJ. 2013;346:f108.

[18] Figueras F, Eixarch E, Meler E, et al. Small-for gestational age fetuses with normal umbilical artery doppler have suboptimal perinatal and neurodevelopmental outcome. Eur J Obstet Gynecol Reprod Biol. 2008;136(1): 34–38.

[19] Rizzo G, Mappa I, Bitsadze V, et al. Role of doppler ultrasound at time of diagnosis of late-onset fetal growth restriction in predicting adverse perinatal outcome: prospective cohort study. Ultrasound Obstet Gynecol. 2020;55(6):793–798.

[20] Caradeux J, Martinez-Portilla RJ, Peguero A, et al. Diagnostic performance of third-trimester ultrasound for the prediction of late-onset fetal growth restriction: a systematic review and meta-analysis. Am J Obstet Gynecol. 2019;220(5):449–459.

[21] Gudmundsson S, Dubiel M, Sladkevicius P. Placental morphologic and functional imaging in high-risk pregnancies. Semin Perinatol. 2009;33(4):270–280.

[22] Lai PK, Wang YA, Welsh AW. Reproducibility of regional placental vascularity/perfusion measurement using 3D power doppler. Ultrasound Obstet Gynecol. 2010;36(2):202–209.

[23] Paules C, Dantas AP, Miranda J, et al. Premature placental aging in term small-for-gestational-age and growth-restricted fetuses. Ultrasound Obstet Gynecol. 2019;53(5):615–622.

[24] Manganaro L, Fierro F, Tomei A, et al. MRI and DWI: feasibility of DWI and ADC maps in the evaluation of placental changes during gestation. Prenat Diagn. 2010;30(12–13):1178–1184.

[25] Javor D, Nasel C, Schweim T, et al. *In vivo* assessment of putative functional placental tissue volume in placental intrauterine growth restriction (IUGR) in human fetuses using diffusion tensor magnetic resonance imaging. Placenta. 2013;34(8):676–680.

[26] Bonel HM, Stolz B, Diedrichsen L, et al. Diffusion-weighted MR imaging of the placenta in fetuses with placental insufficiency. Radiology. 2010; 257(3): 810–819.

[27] Siauve N, Chalouhi GE, Deloison B, et al. Functional imaging of the human placenta with magnetic resonance. Am J Obstet Gynecol. 2015;213(4 Suppl): S103–S114.

[28] Han R, Huang L, Sun Z, et al. Assessment of apparent diffusion coefficient of normal foetal brain development from gestational age week up to term age: a preliminary study. Fetal Diagn Ther. 2015;37(2): 102–107.

[29] Di Trani MG, Manganaro L, Antonelli A, et al. Apparent diffusion coefficient assessment of brain development in normal fetuses and ventriculomegaly. Front Phys. 2019;7:160.

[30] Iima M, Le Bihan D. Clinical intravoxel incoherent motion and diffusion MR imaging: past, present, and future. Radiology. 2016;278(1):13–32.
[31] Derwig I, Lythgoe DJ, Barker GJ, et al. Association of placental perfusion, as assessed by magnetic resonance imaging and uterine artery doppler ultrasound, and its relationship to pregnancy outcome. Placenta. 2013;34(10):885–891.
[32] Capuani S, Guerreri M, Antonelli A, et al. Diffusion and perfusion quantified by magnetic resonance imaging are markers of human placenta development in normal pregnancy. Placenta. 2017;58:33–39.
[33] Slator PJ, Hutter J, McCabe L, et al. Placenta microstructure and microcirculation imaging with diffusion MRI. Magn Reson Med. 2018;80(2):756–766.
[34] Ercolani G, Capuani S, Antonelli A, et al. IntraVoxel incoherent motion (IVIM) MRI of fetal lung and kidney: can the perfusion fraction be a marker of normal pulmonary and renal maturation? Eur J Radiol. 2021; 139:109726.
[35] Lu T, Song B, Pu H, et al. Prognosticators of intravoxel incoherent motion (IVIM) MRI for adverse maternal and neonatal clinical outcomes in patients with placenta accreta spectrum disorders. Transl Androl Urol. 2020;9(2):258–266.
[36] Siauve N, Hayot PH, Deloison B, et al. Assessment of human placental perfusion by intravoxel incoherent motion MR imaging. J Matern Fetal Neonatal Med. 2019;32(2):293–300.
[37] Andescavage N, You W, Jacobs M, et al. Exploring *in vivo* placental microstructure in healthy and growth-restricted pregnancies through diffusion-weighted magnetic resonance imaging. Placenta. 2020;93:113–118.
[38] Jones DK, Basser PJ. "Squashing peanuts and smashing pumpkins": how noise distorts diffusion-weighted MR data. Magn Reson Med. 2004;52(5):979–993.
[39] Sohlberg S, Mulic-Lutvica A, Olovsson M, et al. Magnetic resonance imaging-estimated placental perfusion in fetal growth assessment . Ultrasound Obstet Gynecol. 2015;46(6):700–705.
[40] Jakab A, Tuura RL, Kottke R, et al. Microvascular perfusion of the placenta, developing fetal liver, and lungs assessed with intravoxel incoherent motion imaging. J Magn Reson Imaging. 2018;48(1):214–225.
[41] Chen T, Zhao M, Song J, et al. The effect of maternal hyperoxygenation on placental perfusion in normal and fetal growth restricted pregnancies using intravoxel incoherent motion. Placenta. 2019;88:28–35.
[42] Anderson KB, Hansen DN, Haals C, et al. Placental diffusion-weighted MRI in normal pregnancies and those complicated by placental dysfunction due to vascular malperfusion. Placenta. 2020;91:52–58.
[43] Maiuro A, Antonelli A, Manganaro L, et al. Molecular diffusion and perfusion of biological water quantified by MRI for the diagnosis of pathological human placentas. Il Nuovo Cimento C. 2020;43(4–5):1–5.
[44] Parra-Saavedra M, Crovetto F, Triunfo S, et al. Added value of umbilical vein flow as a predictor of perinatal outcome in term small-for-gestational-age fetuses. Ultrasound Obstet Gynecol. 2013;42(2):189–195.
[45] Kessler J, Rasmussen S, Godfrey K, et al. Fetal growth restriction is associated with prioritization of umbilical blood flow to the left hepatic lobe at the expense of the right lobe. Pediatr Res. 2009;66(1):113–117.
[46] Toutain J, Prochazkova-Carlotti M, Cappellen D, et al. Reduced placental telomere length during pregnancies complicated by intrauterine growth restriction. PLOS One. 2013;8(1):e54013.
[47] Biron-Shental T, Sadeh-Mestechkin D, Amiel A. Telomere homeostasis in IUGR placentas – a review. Placenta. 2016;39:21–23.
[48] Parra-Saavedra M, Crovetto F, Triunfo S, et al. Placental findings in late-onset SGA births without doppler signs of placental insufficiency. Placenta. 2013;34(12):1136–1141.
[49] Salavati N, Smies M, Ganzevoort W, et al. The possible role of placental morphometry in the detection of fetal growth restriction. Front Physiol. 2018;9:1884.
[50] Veerbeek JH, Nikkels PG, Torrance HL, et al. Placental pathology in early intrauterine growth restriction associated with maternal hypertension. Placenta. 2014;35(9):696–701.
[51] Melbourne A, Aughwane R, Sokolska M, et al. Separating fetal and maternal placenta circulations using multiparametric MRI. Magn Reson Med. 2019; 81(1):350–361.